FLOW CONTROL IN SERPENTINE INLET DUCT USING VORTEX GENERATOR JETS

Sushant Chandra, M.C. Keerthi, A. Kushari and R.K. Sullerey
Department of Aerospace Engineering
Indian Institute of Technology Kanpur
Kanpur-208 016, India
Email : akushari@iitk.ac.in

Abstract

The objective of the present research is to study the effectiveness of steady and pulsed vortex generator jets in reducing inlet flow distortion and in improving pressure recovery by effective secondary flow control in uniform inflow serpentine duct diffuser. The measurements were carried out at a test Reynolds number of 6.5 x 10^5 based on the diffuser inlet width. Serpentine duct diffuser consisted of two main portions, namely, a square to circular constant area transition duct followed by a circular diffusing duct. Investigations show that the flow in the serpentine diffusing duct suffers from stall on the inner wall and consequently the outflow at AIP has considerable flow distortion due to the combined effect of secondary flow and the inner wall stall. It is observed that the use of vortex generator jets, both in steady and pulsed modes, improve the performance substantially. The number of jets, location of jets, velocity ratios and the pulse frequency are some of the variables that are studied. The results obtained so far suggest that use of pulsed jet not only gives better performance but also reduces the amount of air that is needed to be injected through the jets in comparison to steady jets for similar velocity ratios.

Keywords: *Serpentine duct, flow control, pulse jets*

Nomenclature

c_f* = Indicative skin friction coefficient
c_p = Mass-averaged static pressure coefficient
L = Linear duct length in streamwise direction
p_0 = Total pressure
v = Fluid velocity
P_{AV} = Average of total pressure values at a given radial location at exit plane
P_{AV-LOW} = Average of total pressure values below P_{AV} at a given radial location at exit plane
x = Linear distance from the duct inlet along streamwise direction
ρ = Air density
χ = Velocity ratio w.r.t. duct inlet freestream velocity
ψ = Mass flow rate ratio w.r.t. duct inlet mass flow rate
ω = Total pressure loss coefficient
AIP = Aerodynamic interface plane
DE = (circumferential) distortion extent
DI = (circumferential) distortion intensity
VGJ = Vortex generator jets

Subscripts

1 = Duct inlet plane value
2 = Duct exit plane value
∞ = Freestream value at duct inlet (reference for all pressure measurements)
av = Average of values at duct exit plane
j = Vortex generator jets parameter
w = Value measured at the duct wall

Introduction

Serpentine inlet ducts are so called because they have a double-S shape that gives them a snake like appearance. They are used in applications with design focus on a short and compact intake with a stealth enhancement require-

Paper Code : V64 N3/758-2012. Manuscript received on 05 Sep 2011. Reviewed and accepted as a Full Length Contributed Paper on 11 Jun 2012

ment. The compact nature of the duct limits the length for diffusion and, this, combined with rapid turning, leads to complex three dimensional flows involving separation and secondary flows. These result in highly distorted flow at the Aerodynamic Interface Plane (AIP) between the intake and the compressor and the engine face distortion can cause a reduction in stability margin for the compressor.

There have been numerous studies of the flow through a serpentine duct reported in open literature. Brear et al [1] carried out an experimental and computational study of a serpentine inlet for an Uninhabited Combat Air Vehicle. The study indicated that separation from the top surface of the inlet was the dominant phenomenon and resulted in large unsteady flow structures. These structures caused a drop in inlet pressure recovery and increased inlet unsteadiness. Rabe [2] conducted an experimental investigation to determine the effectiveness of a serpentine inlet duct with active flow control for two simulated flight conditions. The flow control was achieved by using air injection through micro jets at 1% of the inlet mass flow rate. The inlet duct was tested at cruise condition and at an angle of attack to determine the change in inlet performance due to flow control at different flight conditions. It was observed that the use of flow control enabled the compressor to recover a significant portion of the undistorted stability margin.

There are many studies on control of secondary flows and separation by passive and active means [3-8]. Reichert and Wendt [3] investigated the performance of diffuser using low profile vortex generators and tapered fin type vortex generators. Their studies showed improvement in diffuser performance by using the above techniques which rely on efficient control of secondary flows. Pradeep and Sullerey [9] have investigated the use of vortex generators in circular and transitioning S-duct diffusers. It was observed that vortex generator jets could be used for control of both separation as well as secondary flows. The jet to free stream velocity ratio and the number of jets and their locations were important parameters. Hansen and Bons [10] have investigated the effect of pulsed vortex generator jets in controlling the separation of boundary layers.

The present experimental investigations are carried out in a more complex flow field of a serpentine duct that has both a transitioning and a diffusing section, both with high curvatures. The study is aimed to quantify the effectiveness of vortex generator jets with and without pulsing in control of a serpentine duct flow. The performance has been evaluated for a range of jet to free stream velocity ratios, jet locations and pulse frequencies. The performance parameters measured and evaluated include total pressure loss, pressure recovery and flow distortions at the aerodynamic interface plane as per SAE ARP-1420 [11] guidelines.

Experimental Setup and Procedure

The experiments were carried out in a low speed wind tunnel with a square exit of side 306 mm. The exit plane was preceded by a straight duct of length 300 mm to obtain a zero pressure gradient turbulent boundary at the inlet. The mean flow velocity was 31 m/s and the corresponding Reynolds number based on the diffuser inlet width was 6.5 x 10^5. The inlet turbulence level was 0.1%.

The serpentine duct geometry is shown in Fig.1. It comprised of a square to a circular transitioning duct (radius of curvature ratio with respect to the inlet side length of 4) followed by a diffuser section (radius ratio 6), with each section followed by a straight portion for stabilization of flow properties.

Figure 2 shows the arrangement of the VGJs (vortex generator jets) in the test model. The pitch and skew angles (45° and 135°) of vortex generator jets were retained as reported by Pradeep and Sullerey [9]. Fig.3 shows the VGJ defining angles with reference to the secondary flow. Three circumferential arrays of vortex generator jets were placed along the inner wall at axial locations: location 1 corresponded to the location of maximum wall normal pressure gradient and two more locations (locations 2 and 3) upstream of separation point, respectively. Jets were placed at location 1 at an angular separation of 30°, symmetrically about the wall centerline. At the locations 2 and 3 the angular separation between the jets was reduced to 15° so as to accommodate more number of jets within the same sector angle.

The air supply for the vortex generator jets was drawn from a compressed air source. The supply circuit is shown in Fig.4. An air flow meter was used to measure the flow rate of air to the vortex generator jets. The placement of jets and their numbers have been varied as a part of this study. Additionally, four solenoid valves along with 12V DC power source and function generator are used for pulsed vortex generator jets. The details of the experimental setup, instrumentation, calibration and measurements can be found in [12].

A digital multi-channel micro-manometer with 0.01% full scale calibration accuracy (FCO510 from Furness Controls®) was used for all pressure measurements. Altogether, this set-up for c_p measurement had an error of about ±1% (as determined from analysis of 30 repeated observations at one point). The skin friction coefficient (c_f*) was obtained using Preston tubes placed at multiple locations on the wall to ascertain the location of separation point. Total pressure measurements at the outflow plane (AIP) were carried out with a Kiel probe (uncertainty limit of ±1% for a confidence level of 95% [12]).

In order to compare the performance of the serpentine duct under various flow control configurations, a set of consistent performance parameters are needed. All pressure measurements were made with reference to the inlet free stream static port pressure. A modified definition (based on the one given by Nicoll and Ramaprian [13]) of static pressure coefficient c_p was used here to incorporate the effects of the added mass flows, as

$$c_p = \frac{(p - p_\infty)(1 + \psi_i)}{\frac{1}{2}\rho v_\infty^2 (1 + \psi_j \chi_j^2)}$$

A non-dimensional total pressure loss coefficient at a given point in the exit plane, or the aerodynamic interface plane (AIP), is defined as

$$\omega = \frac{p_{0\infty} - p_{02}}{\frac{1}{2}\rho v_\infty^2}$$

The Society of Aerospace Engineer's Aerospace Recommended Practice (SAE-ARP) 1420 [11] provides guidelines by which gas turbine engine aerodynamic stability and performance can be evaluated, as influenced by the quality of airflow delivered to the engine. The distortion descriptors used here are the circumferential distortion intensity and extent. These definitions are based on a prescribed grid for measurement, which consists of points on five equal area annuli further divided into eight similar sectors each subtending an angle of 45. The definitions for the circumferential distortion intensity (DI) and extent (DE) used for the present study are from SAE-ARP 1420 [11]. The circumferential distortion intensity is defined as

$$DI = \frac{P_{AV} - P_{AV-LOW}}{P_{AV}}$$

The circumferential distortion extent is the sector angle over which the local total pressure is less than the ring-average total pressure.

Initial experiments carried out with different jet locations [12] indicated that the results are most promising with location 2 and therefore results are presented here for only that location.

Results and Discussion

Initially the test was conducted on bare duct (i.e. duct without flow control) thereafter steady and pulsed vortex generator jets were used and the performance of the diffuser was evaluated. Investigations show that the flow in the serpentine diffusing duct suffers from stall on the inner wall and the outflow at AIP has considerable flow distortion due the combined effect of secondary flow and the inner wall stall. It is observed that the use of vortex generator jets both in steady and pulsed modes improves the performance.

Figure 5 presents the wall static pressure distribution for the bare duct along the non-dimensional wall length (x is the distance along the duct centerline and L is the total duct length). The location of maximum pressure differential between the two walls is where the secondary flow starts building up and combined with subsequent adverse pressure gradient leads to flow separation and flow distortion. The location of control jets is therefore kept downstream of the location of the maximum pressure differential which is at x/L=0.37.

A performance comparison with steady and pulsed vortex generator jets is shown in Table-1. For sake of comparison, the velocity ratio VR (not exactly same) and number of jets and their locations are maintained identical. The results presented are for a pulse frequency of 8 Hz. Pulse frequency of 8 Hz was an optimum value as either decrease or increase of frequency lowered the performance [12]. The static pressure coefficient (c_p) is defined based on difference of circumferential averaged static pressure at AIP and the inlet static pressure normalized with inlet dynamic head. It can be noted that with both the steady and the pulsed jet vortex generators, the performance of the serpentine duct diffuser improves significantly. There was a 9.2% improvement in total pressure loss coefficient in case of steady blowing and 11.6 % improvement with pulsed jets with respect to the bare duct. The static pressure coefficient improved by about 93% with both the control schemes. However with pulsed jets, there

Table-1 : A Comparison of Steady and Pulsed Jets

	Bare Duct	Steady VR=2.5	Pulsed VR=2.57
Static pressure coefficient	0.058	0.112	0.112
Total pressure loss coefficient	0.689	0.625	0.609
Distortion intensity	0.464	0.44	0.30
Distortion extent	189°	196°	187°
Mass fraction (%)	0.0	0.132	0.07

Table-2 : Effect of Velocity Ratio on Performance

	VR=1.2	VR=2.5	VR=5.7	VR=7.7
Static pressure coefficient	0.101	0.112	0.136	0.141
Total pressure loss coefficient	0.646	0.625	0.559	0.542
Distortion intensity	0.214	0.210	0.195	0.185
Distortion extent	192°	196°	192°	208°
Mass fraction (%)	0.065	0.137	0.306	0.412

was a substantial drop of 35.3% in the distortion intensity [11] as opposed to only 5.1% drop with steady vortex generating jets as compared to the bare duct. On the other hand, the use of steady jets increased the extent of distortion to up to 196° as compared to 189° for bare duct. It can be concluded that with pulsed vortex generating jets, the improvements are greater, and more over the mass fraction of air required through the jets is significantly reduced (to 0.07%) for pulsed jets as compared to the steady jet (0.13%).

Table-2 presents the effect of velocity ratio on performance of serpentine duct with steady vortex generator jets. It is observed that performance improves with the increase in the velocity ratio. However the injected mass flow requirement also increases in proportion to the increase in the velocity ratio. The gains in performance are less as the velocity ratio increases. Due to limitation of flow rate through the valves, a similar study could not be carried out with the pulsed jets.

Figure 6 shows the streamwise distribution of skin friction coefficient at the inner wall for the bare duct and with pulsed vortex generating jets. It can be observed that the separation is delayed (to X/L = 0.47) for the case of pulsed jet compared to the bare duct in which the separation occurred at X/L = 0.37.

The total pressure recovery contours for the bare duct and for duct with steady vortex generator jets with velocity ratio of 7.7 are shown in Figs.7 and 8 respectively. Four jets are used in location 2. Significant improvement can be observed in areas of initially low total pressures with the employment of vortex generator jets.

A comparison of total pressure recovery contours for similar velocity ratios for steady and pulsed jet can be made by observing Figs.9 and 10. The pulse frequency was 8 Hz. It can be noted that with pulse jets, there was an improvement in total pressures in regions of low total pressures with the steady jets.

Conclusions

An experimental study on flow control in serpentine duct diffusers has been carried out using steady and pulsing vortex control jets. The results indicate a significant improvement in performance with both steady and pulsing jets. It is observed that for same jet to free stream velocity ratios, pulsing jets give better performance as compared to steady jets. Further, the jet mass flow required with pulsing jets is less than with the steady jets. In steady jets, improved performance was also observed with increase in jet to free stream velocity ratios.

Acknowledgement

This project was sponsored by the Aerodynamics Panel of Aeronautical Research and Development Board.

References

1. Brear, M.J., Warfield, Z., Mangus, J.F., Braddom, C.S., Paduano, J.D. and Philhower, J.S. , "Flow Separation within the Engine Inlet of an Uninhabited Combat Air Vehicle (UCAV)", Proceedings of the 4th ASME/JSME Joint Fluids Engineering Conference, 2003, Honolulu, Hawaii.

2. Rabe, A.S., "Effectiveness of a Serpentine Inlet Duct Flow Control Technique at Design and Off-Design Simulated Flight Conditions", ASME J. Turbomachinery, Vol.128, No.2, pp.332-339, 2006.

3. Johnston, J. P. and Nishi, M., "Vortex Generator Jets-Means for Flow Separation Control", AIAA Journal, Vol. 28, No. 6, pp. 989-994, 1990.

4. Reichart, B.A. and Wendt, B.J., "Improving Curved Diffuser Performance with Vortex Generators", AIAA Journal, Vol. 34, No. 1, pp.65-72, 1996.

5. Kwong, A.H.M. and Dowling, A.P., "Active Boundary Layer Control in Diffusers", AIAA Journal, Vol.32, pp. 2409-2414, 1994.

6. Harper, D.K., Leitch, T.A., Ng, W.F. and Guillot, S.A., "Boundary-Layer Control and Wall-Pressure Fluctuations in a Serpentine Inlet", Proceedings of the AIAA/ASME/ASEE Joint Propulsion Conference, 2000.

7. Hamstra, J.W., Miller, D.N., Truax, P.P., Anderson, B.A. and Wendt, B.J., "Active Inlet Flow Control Technology Demonstration", Aeronautical Journal, Vol. 104, pp. 473-479, 2000.

8. Sullerey, R.K., Mishra, S. and Pradeep, A.M., "Performance Improvement of S-Duct Diffusers", ASME J. Fluids Eng., Vol. 124, pp. 136-142, 2002.

9. Pradeep, A.M. and Sullerey, R.K., "Active Flow Control in Circular and Transitioning S-Duct Diffusers ", ASME, J. of Fluids Eng., Vol. 128, No. 4, pp. 1192-1203, 2006.

10. Hansen, L. C. and Bons, J. P., "Phase-Locked Flow Measurements of Pulsed Vortex-Generator Jets in a Separating Boundary Layer", AIAA Journal of Propulsion and Power, Vol. 22, No. 3, pp. 558-566, 2006.

11. SAE, 1973, "Aerospace Recommended Practices", ARP-1420.

12. Chandra, S., "Effectiveness of a Serpentine Inlet Duct Control Scheme", M. Tech. Thesis, Department of Aerospace Engineering, Indian Institute of Technology Kanpur, 2008.

13. Nicoll, W. B. and Ramaprian, B. R., "Performance of Conical Diffusers With Annular Injection at Inlet", Journal of Basic Engineering, Vol. 92, 1970.

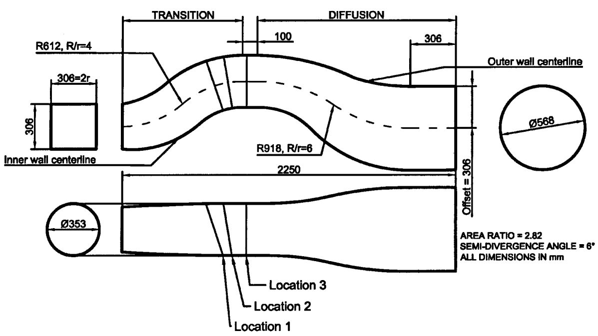

Fig.1 Serpentine Inlet Duct Geometry Showing the Location of VGJ's

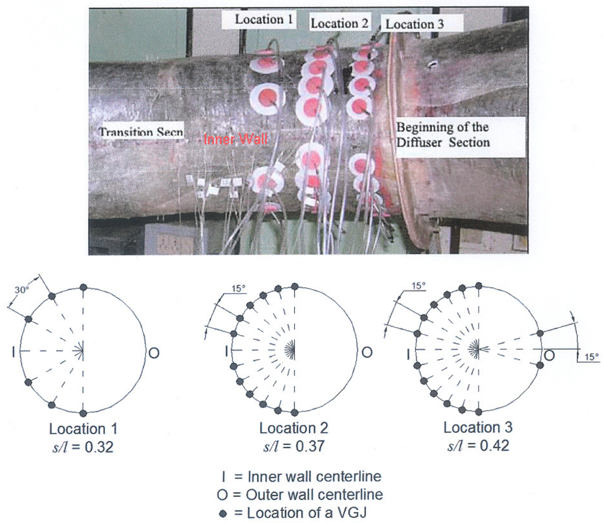

Fig.2 Vortex Generator Jet Locations

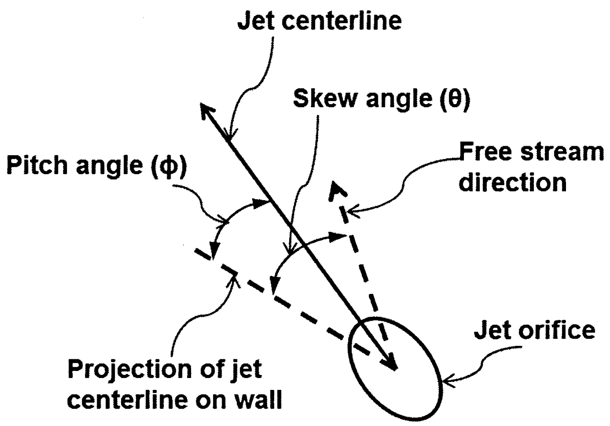

Fig.3 Vortex Generator Jet Angles

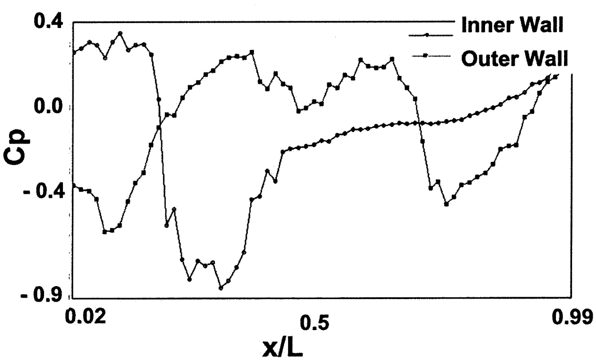

Fig.5 Wall Static Pressure Distribution for Bare Duct

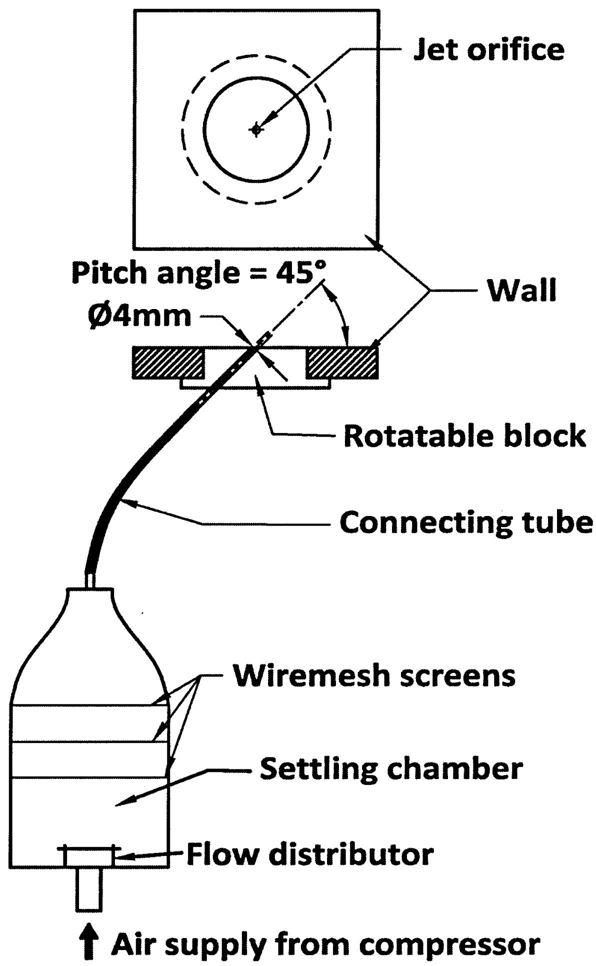

Fig.4 Air Circuit for Vortex Generator Jets

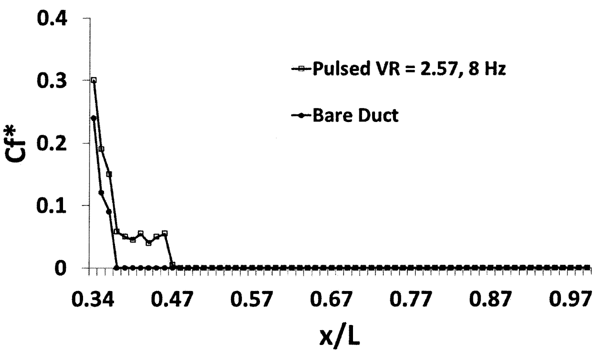

Fig.6 Streamwise Variation of Skin Friction Coefficient on the Inner Wall

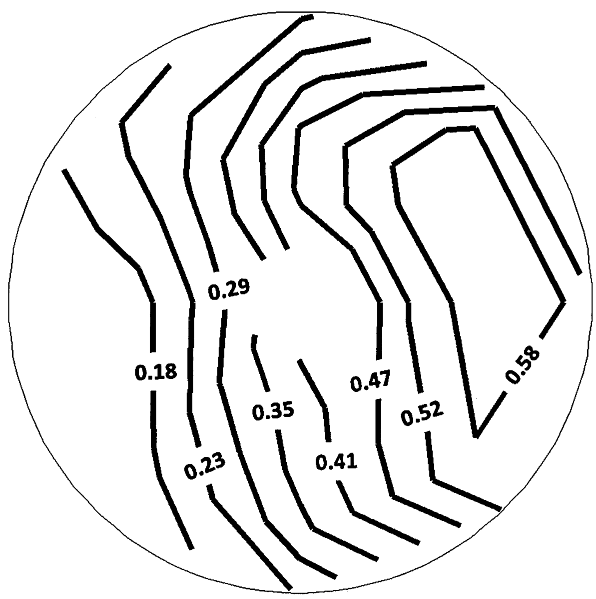

Fig.7 Total Pressure Recovery Contours of Bare Duct

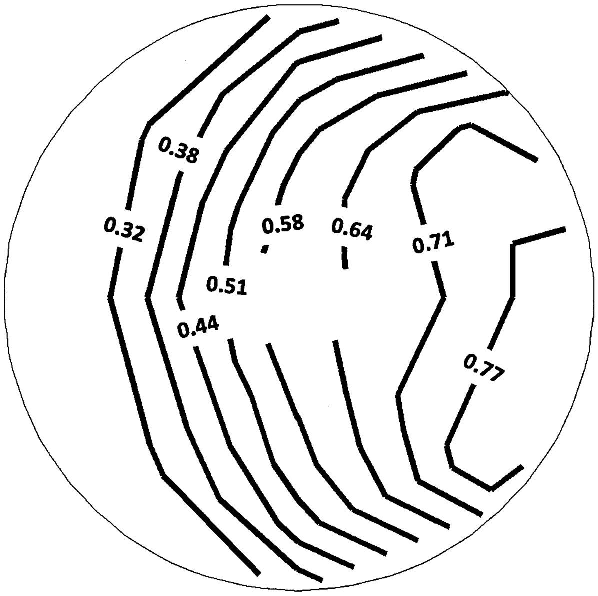

Fig.8 Total Pressure Recovery Contours for Steady Jet with VR = 7.7

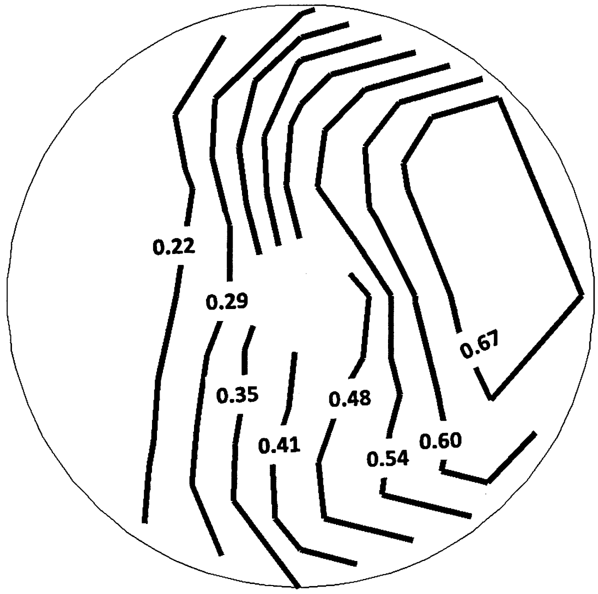

Fig.9 Total Pressure Recovery Contours (Steady Jet) for VR = 2.5

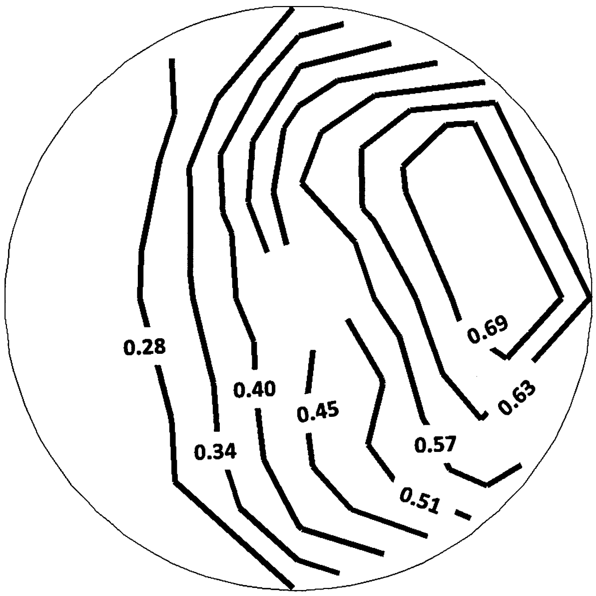

Fig.10 Total Pressure Recovery Contours (Pulsed Jet) for VR = 2.57